Optimization of Wastewater Treatment of Hydraulic Fracturing Fluids via Modeling and Simulation of Anaerobic Digestion and Depolymerization

The batch bioreactor was coded in C++, and then compiled in R using the R package *mrgsolve*. Currently available model inputs include temperature, initial biomass concentrations, headspace allocation, and number of oil wells to pull from. Partial differential equations (PDEs) were developed to keep track of bacteria growth, contaminant depletion, intermediate product peak concentrations/depletion time, and pressure accumulation due to the formation of biogas. The PDEs present in the model. The PDEs rely on kinetic data based on either the Monod equation, or Michaelis-Menten kinetics, and are organized by their respective bioprocess in Appendix E. Derivations of each PDE are summarized below. For the full list of PDEs that govern the model, see the *Mathematical Model* Tab.

Hydrolysis of guar gum involves depolymerizing complex polysaccharide chains into monomeric units galactose and mannose, which are both $C_6H_{12}O_6$ (with different structures), as seen in figure 1.

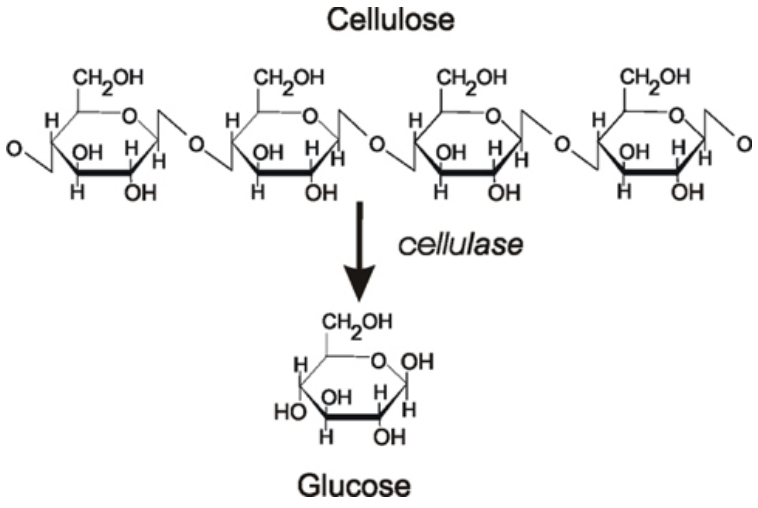

Figure 1: Example of enzymatic hydrolysis breaking polysaccharide chains [5].

Guar gum is a complex polysaccharide with a mannose backbone and galactose side chains in a ~ 1.6:1 to 2:1 ratio (M:G) [5]. Realistically this step would result several different monomers, yet since both structures have the same chemical

formula ($C_6H_{12}O_6$), it was assumed that only glucose was formed in order to simplify the problem. Additionally, enzymatic hydrolysis would create side products, such as hydrogen or water, though this will be ignored to as well, as stoichiometric equations attempting to summarize this process are often poor estimations of the actual yield or not provided. The hydrolysis of guar gum was modeled using a modified Michaelis-Menten formula, as seen in equation 1 [5].

$$\frac{dL}{dt} = -\left(\frac{k_{cat} * C_e * L}{K_m + L}\right), \qquad k_{cat} = {}^{v_{max,G}}/_{C_e} \qquad (1)$$

Where k_{cat} is the reaction rate, k_m is the Michaelis-Menten constant, C_e is effective enzyme concentration (reported in unit/mL polymer), and L is the molar concentration of cleavable bonds in the system. The enzyme identified for this process is ß-mannanase, at a concentration of 0.002 units/mL guar gum. Though C_e is not technically a concentration, as it scales with the remaining volume of guar gum, it approximates the experimental data relatively well [5]. The number of cleavable bonds per mole (N_{Bonds}) was assumed to be equal to the molecular weight of guar gum (~1,200,000 g/mol) divided by the molecular weight of glucose (180 g/mol), which is approximately equal to 6600. The initial molar concentration of guar gum was multiplied by N_{Bonds}, or 6600 bonds per mole. The overall stoichiometry for enzymatic hydrolysis was then assumed to follow equation 2.

$$(C_6H_{12}O_6)_n \rightarrow n(C_6H_{12}O_6) \qquad (2)$$

While glucose is being formed through hydrolysis, it is simultaneously being fermented into one of three intermediate products. Acidogenesis and some acetogenic reactions work to ferment glucose further into more readily available intermediate products. Again in reality, many products may be formed here. Most kinetic models choose a few intermediates that are most likely to form based on the substrate. Propanoic acid and ethanol arise more frequently in the literature and were chosen for this model [13]. As the name suggests, only acidogenesis is responsible for creating the above intermediates, as Acetogenesis solely forms acetate. The purpose of acidogenesis is to break the monomeric units, i.e. glucose, into VFA's or useable chains as seen in Figure 2. Below are the two acidogenic reactions and the single acetogenic reaction responsible for fermenting glucose.

Ethanol Formation: $C_6H_{12}O_6 \leftrightarrow 2CH_3CH_2OH + 2CO_2$ (3)

Propanoic Acid Formation: $C_6H_{12}O_6 + 2H_2 \leftrightarrow 2CH_3CH_2OOH + 2CO_2$ (4)

Acetic Acid Formation: $C_6H_{12}O_6 \rightarrow 3CH_3COOH$ (5)

These reactions were modeled using the Monod equation. For reference, the Monod equation assumes a bacterial growth rate proportional to the substrate utilization rate. Conversely, Michaelis-Menten kinetics assumes a constant enzyme or bacteria concentration. However, Michaelis-Menten type kinetics can be normalized with concentration, as was done in the hydrolysis reaction rate in Equation 1.

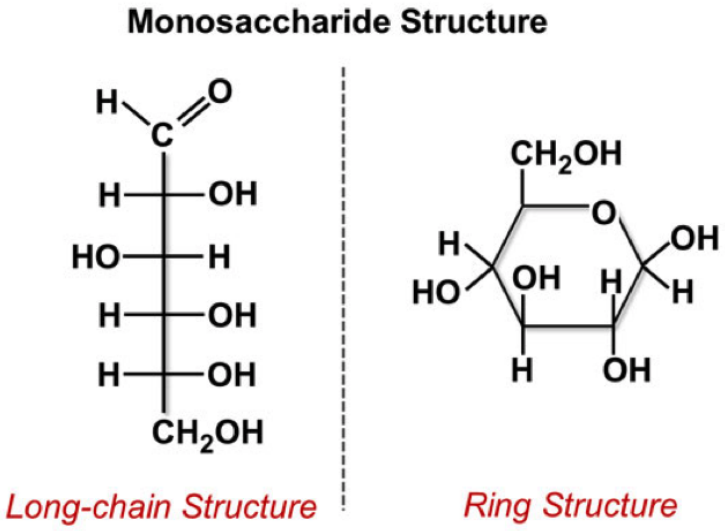

Figure 2: Example of acidogenesis breaking of monosaccharide ring structure. Note that the chain structure is broken down further according to the acidogenic reactions [14].

Application of the Monod equation can be seen in Equations 6 to 8, where μ_{max} is the max growth rate for the bacteria on the substrate, μ is the current growth rate, Ks is the half-saturation constant of the substrate, X is the biomass concentration in g/L, Y is the yield in gram biomass per gram substrate, and S is the substrate concentration.

Substrate: $\frac{dS}{dt} = -(\mu * X) = -\left(\frac{\mu_{max} * S}{Ks+S}\right) * X$ (6)

Biomass: $\frac{dX}{dt} = -Y * \frac{dS}{dt}$ (7)

Combined: $\frac{dS}{dt} = -\frac{1}{Y}\frac{dX}{dt} = -\left(\frac{\mu_{max} * S}{Ks+S}\right) * \frac{X}{Y}$ (8)

The three remaining acetogenic reactions utilize ethanol, propanoic acid, and both H_2 and CO_2 gas as substrates. The digestion of ethanol and propanoic acid are again modeled using the Monod equation, however the consumption of H_2 gas was modeled using normalized Michaelis-Menten kinetics, as seen in Equation 9.

$$v = \frac{d[H_2]}{dt} = \frac{v_{max}([H_2]-[H_2]^*)}{Km+ [H_2]-[H_2]^*} \quad (9)$$

Here, $[H_2]$ is partial pressure in pascals, $[H_2]^*$ is the threshold pressure specific to the acetobacterium or methanogen, v_{max} is the consumption rate of H_2 in nmol/h, and Km is the Michaelis-Menten constant in pascals. This equation is normalized with biomass concentration. $[H_2]^*$ is 55 pascals for acetobacterium *A. bakii* [15]. The following reactions govern the rest of the Acetogenesis stage.

$$CH_3CH_2OH + 2H_2O \leftrightarrow CH_3COOH + 3H_2 \quad (10)$$

$$CH_3CH_2COOH + 3H_2O \leftrightarrow CH_3COOH + 3H_2 + CO_2 + H_2O \quad (11)$$

$$2CO_2 + 4H_2 \rightarrow CH_3COOH + 2H_2O \quad (12)$$

Methanogenesis is modeled the same way Acetogenesis is, in that both Monod and normalized Michaelis-Menten kinetics were utilized. Here, $[H_2]^*$ is 1 pascal for methanogen strain MSB [15]. In this step, acetate, hydrogen gas, and some CO2 are converted to methane, water, and more CO2. The two reactions being modeled are as follows:

$$CO_2 + 4H_2 \rightarrow CH_4 + 2H_2O \quad (13)$$

$$CH_3COOH \rightarrow CH_4 + CO_2 \quad (14)$$

To provide deeper insight into mathematics behind the model, Equation 15 is shown below as an example of one of the PDEs derived using Monod parameters.

$$\frac{d(Ethanol)}{dt} = \frac{dE}{dt} = \begin{bmatrix} Stoich\left(\frac{\mu_{max,G} * C_{Glucose}}{Ks_G + C_{Glucose}} * \frac{X_{Acidogen}}{MW_{Glucose} * Y_{Acidogen}}\right) \\ -Stoich\left(\frac{\mu_{max,E} * C_{Ethanol}}{Ks_E + C_{Ethanol}} * \frac{X_{Acetogen}}{MW_{Ethanol} * Y_{Acetogen}}\right) \end{bmatrix} * vol \quad (15)$$

Where $C_{Ethanol}$ is the molar concentration of ethanol (mol/L), MW_i is the molecular weight of the substrate, Y_i is the yield in grams biomass per gram substrate, *vol* is the liquid volume in the reactor in liters, X_i is the biomass concentration in g/L, E is the total accumulation of moles of ethanol, and *Stoich* is the stoichiometric coefficient. See Appendix E for the full list of differential equations used in the model.

References

[1] US Congress. Energy Policy Act of 2005. Section 322.

[2] Kondash, Andrew; Albright, Elizabeth; Vengosh, Avner. (2016). “Quantity of flowback and produced waters from unconventional oil and gas exploration”. Science of Total Environment. Vol 574: pg 314-321.

[3] “Hydraulic Fracking Disclosure.” Find a Well | FracFocus Chemical Disclosure Registry, fracfocusdata.org/.

[4] Iowa Rural Water Association. “Bacteria and Protozoa - Tips and Tools” (2019).

[5] Cheng, Y., and R. K. Prud'homme. "Enzymatic Degradation of Guar and Substituted Guar Galactomannans." Biomacromolecules, vol. 1, no. 4, 2000, pp. 782-788.

[6] Y. Geng et al., "Biodegradation of isopropanol by a solvent-tolerant Paracoccus denitrificans Strain" (2015). Prep Biochem Biotechnology, vol. 45, no. 5, pp. 491-499.

[7] Y. Tucker, J. Kotcon, and T. Mroz, "Methanogenic Archaea in Marcellus Shale: A Possible Mechanism for Enhanced Gas Recovery in Unconventional Shale Resources" (2015). Environmental Science & Technology, vol. 49, no. 11, pp. 7048-7055.

[8] J. Galagan, "The Genome of M. acetivorans Reveals Extensive Metabolic and Physiological Diversity" (2002). Genome Research, vol. 12, no. 4, pp. 532-542.

[9] US EPA, "Biosolids Technology Fact Sheet - Multi-Stage Anaerobic Digestion", US EPA, (2006).

[10] D. Lipus, "MICROBIOLOGY OF HYDRAULIC FRACTURING WASTEWATER" (2017). Doctorate of Philosophy, Swanson School of Engineering, University of Pittsburgh.

[11] Naim, M., Elewa, M., El-Shafei, A., & Moneer, A. (2015). Desalination of simulated seawater by purge-air pervaporation using an innovative fabricated membrane. Water Science and Technology, 72(5), 785-793.

[12] Abraham, J., Vasu, K. S., Williams, C. D., Gopinadhan, K., Su, Y., Cherian, C. T., . . . Nair, R. R. (2017). Tunable sieving of ions using graphene oxide membranes.Nature Nanotechnology, 12(6), 546-550.

[13] Moletta, R., D. Verrier, and G. Albagnac. "Dynamic Modelling of Anaerobic Digestion." Water Research, vol. 20, no. 4, 1986, pp. 427-434.

[14] Ogidanrilwan, and Steemkitchen (55). “ROLES OF CARBOHYDRATES IN THE BODY - Steemit.”- Steemit, steemit.com/food/@ogidanrilwan/roles-of-carbohydrates-in-the-body.

[15] Kotsyurbenko, Oleg R., et al. “Competition between Homoacetogenic Bacteria and Methanogenic Archaea for Hydrogen at Low Temperature.” FEMS Microbiology Ecology, vol. 38, no. 2-3, 2001, pp. 153–159

[16] Augusta Sulfate Company, LLC. “Ammonium sulfate SDS”. (2017) [online] http://ictulsa.com/wp-content/uploads/2018/01/AmsulAugusta.pdf

[17] US EPA, “2015 GHGRP Industrial Profiles - Waste” (2015).

[18] Drilling Maps. “Haynesville-Bossier”. (2019). [online] https://www.drillingmaps.com/Haynesville-Bossier.html

[19] Fernández, F. J., J. Villaseñor, and D. Infantes. "Kinetic and Stoichiometric Modelling of Acidogenic Fermentation of Glucose and Fructose." Biomass and Bioenergy, vol. 35, no. 9, 2011, pp. 3877-3883.
[20] Kim, In S., James C. Young, and Henry H. Tabak. "Kinetics of Acetogenesis and Methanogenesis in Anaerobic Reactions Under Toxic Conditions." Water Environment Research, vol. 66, no. 2, 1994, pp. 119-132.
[21] Felchner-Zwirello, Monika. (2014). Propionic Acid Degradation by Syntrophic Bacteria During Anaerobic Biowaste Digestion. Propionic Acid Degradation by Syntrophic Bacteria During Anaerobic Biowaste Digestion. 1-152. 10.5445/KSP/1000037825.
[22] Barthakur, Archana, Munindra Bora, and H. D. Singh. "Kinetic Model for Substrate Utilization and Methane Production in the Anaerobic Digestion of Organic Feeds." Biotechnology Progress, vol. 7, no. 4, 1991, pp. 369-376.
[23] Kettle, Helen. “Modelling Microbial Populations [R Package MicroPop Version 1.4].” The Comprehensive R Archive Network, Comprehensive R Archive Network (CRAN), CRAN.R-project.org/package=microPop.